molecular pharmaceutics

Article

pubs.acs.org/molecularpharmaceutics

Evaluation of ^{89}Zr-pertuzumab in Breast Cancer Xenografts

Bernadette V. Marquez,[†] Oluwatayo F. Ikotun,[†] Alexander Zheleznyak,[†] Brian Wright,[†] Amrita Hari-Raj,[†] Richard A. Pierce,[‡] and Suzanne E. Lapi*[,†]

[†]Mallinckrodt Institute of Radiology, Washington University School of Medicine, Campus Box 8225, 510 South Kingshighway Boulevard, St. Louis, Missouri 63110, United States

[‡]Department of Medicine, Pulmonary and Critical Care Division, Washington University School of Medicine, Campus Box 8052, 660 South Euclid Avenue, St. Louis, Missouri 63110, United States

Supporting Information

ABSTRACT: Pertuzumab is a monoclonal antibody that binds to HER2 and is used in combination with another HER2−specific monoclonal antibody, trastuzumab, for the treatment of HER2+ metastatic breast cancer. Pertuzumab binds to an HER2 binding site distinct from that of trastuzumab, and its affinity is enhanced when trastuzumab is present. We aim to exploit this enhanced affinity of pertuzumab for its HER2 binding epitope and adapt this antibody as a PET imaging agent by radiolabeling with ^{89}Zr to increase the sensitivity of HER2 detection in vivo. Here, we investigate the biodistribution of ^{89}Zr-pertuzumab in HER2−expressing BT-474 and HER2−nonexpressing MDA-MB-231 xenografts to quantitatively assess HER2 expression in vivo. In vitro cell binding studies were performed resulting in retained immunoreactivity and specificity for HER2−expressing cells. In vivo evaluation of ^{89}Zr-pertuzumab was conducted in severely combined immunodeficient mice, subcutaneously inoculated with BT-474 and MDA-MB-231 cells. ^{89}Zr-pertuzumab was systemically administered and imaged at 7 days postinjection (p.i.) followed by terminal biodistribution studies. Higher tumor uptake was observed in BT-474 compared to MDA-MB-231 xenografts with 47.5 ± 32.9 and 9.5 ± 1.7% ID/g, respectively at 7 days p.i (P = 0.0009) and blocking studies with excess unlabeled pertuzumab showed a 5-fold decrease in BT-474 tumor uptake (P = 0.0006), confirming the in vivo specificity of this radiotracer. Importantly, we observed that the tumor accumulation of ^{89}Zr-pertuzumab was increased in the presence of unlabeled trastuzumab, at 173 ± 74.5% ID/g (P = 0.01). Biodistribution studies correlate with PET imaging quantification using max SUV (r = 0.98, P = 0.01). Collectively, these results illustrate that ^{89}Zr-pertuzumab as a PET imaging agent may be beneficial for the quantitative and noninvasive assessment of HER2 expression in vivo especially for patients undergoing trastuzumab therapy.

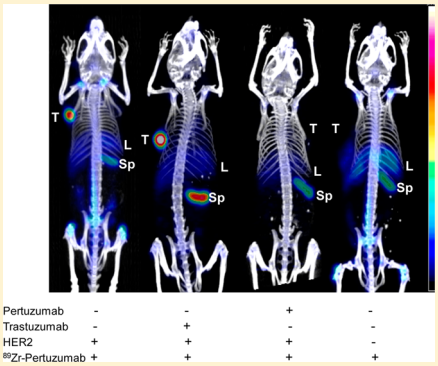

KEYWORDS: *^{89}Zr, pertuzumab, HER2, PET, trastuzumab, breast cancer xenograft, NOG*

INTRODUCTION

^{89}Zr-labeled monoclonal antibodies (mAbs) have recently been useful in clinical trials for positron emission tomography (PET) imaging of various cancers due to the favorable pairing of the radioisotope's half-life ($t_{1/2}$ = 3.3 days) and the antibody's pharmacokinetic properties, complemented by the high sensitivity and quantitative properties of PET.[1−3] Pertuzumab (Perjeta) is an FDA-approved mAb for the treatment of human epidermal growth factor receptor 2 (HER2)-positive metastatic breast cancer, in combination with trastuzumab (Herceptin), another HER2−specific monoclonal antibody. Pertuzumab binds to domain II of the human epidermal growth factor receptor-2 (HER2) epitope, distinct from the trastuzumab epitope located within domain IV. Both antibodies elicit antibody-dependent cellular cytotoxicity (ADCC); however, the predominant mechanisms responsible for the synergy in downregulating HER2 expression are that pertuzumab inhibits HER2 dimerization with other epidermal growth factor receptors and trastuzumab inhibits intracellular signaling.[4]

^{89}Zr-labeled trastuzumab has been evaluated as a PET imaging agent for detecting HER2 expression in trastuzumab-treated or in naïve patients, with promising results toward the stratification of patients mostly likely to respond to trastuzumab therapy.[3,5] However, investigations with pertuzumab as a PET imaging agent have not been explored, to our knowledge. Pertuzumab has only been investigated in vivo as a SPECT imaging agent by radiolabeling with ^{111}In and ^{177}Lu.[6−8] However, the sensitivity of PET imaging may be advantageous for further developing pertuzumab as an imaging agent. A qualitative comparison of fluorescently labeled Cy5-trastuzumab and Cy5-pertuzumab in the presence and absence of either unconjugated trastuzumab or pertuzumab has been conducted

Special Issue: Positron Emission Tomography: State of the Art

Received: April 30, 2014
Revised: July 18, 2014
Accepted: July 24, 2014
Published: July 24, 2014

in HER2+ xenograft models, which suggests imaging with Cy5-pertuzumab in the presence of unconjugated trastuzumab and imaging with Cy5-trastuzumab in the presence of unconjugated pertuzumab do not alter the tumor accumulation of each Cy5-labeled antibody.[9] However, a quantitative comparison between the tumor accumulation of radiolabeled trastuzumab and pertuzumab as imaging agents during trastuzumab therapy has yet to be investigated. Furthermore, in silico studies suggest the binding of trastuzumab induces a change of HER2 conformation, permitting greater exposure of the pertuzumab binding site and enhancing pertuzumab affinity.[10] Toward this end, we investigated ^{89}Zr-pertuzumab in HER2−expressing and nonexpressing breast cancer xenografts. Herein, we demonstrate the specificity of ^{89}Zr-pertuzumab in HER2+ tumors in vivo and quantitatively show enhanced tumor accumulation of ^{89}Zr-pertuzumab in the presence of trastuzumab.

MATERIALS AND METHODS

Reagents and Cell Cultures. Pertuzumab (Perjeta) and trastuzumab (Herceptin) were purchased from Roche (South San Francisco, CA). Desferrioxamine-*p*-benzyl-isothiocyanate (DFO-Bz-NCS) was purchased from Macrocyclics (Dallas, TX). The automated production of ^{89}Zr-oxalate was carried out in house,[11] adapted from previously established methods[12,13] and neutralized to pH 6.8−7.2 as previously developed for optimal radiolabeling.[14] All other chemicals were purchased from Sigma-Aldrich (St. Louis, MO) unless stated otherwise. HER2−expressing breast cancer cell lines BT-474 and SKBR3 as well as HER2−nonexpressing MDA-MB-231 were purchased from the American Type Culture Collection (ATCC, Manassas, VA) and cultured in Iscove's Modified Dulbecco's Medium (IMDM) containing 10% fetal bovine serum (FBS) and 50 μg/mL gentamycin (complete media) in a humidified incubator with 5% CO_2 at 37 °C. Reagents for cell culture were purchased from Life Technologies (Grand Island, NY) unless stated otherwise.

Conjugation and Radiolabeling. Conjugation of DFO-Bz-NCS to pertuzumab and subsequent radiolabeling with ^{89}Zr-oxalate were performed following previous methods.[14−16] Briefly, pertuzumab (10 mg/mL) was conjugated to 8-fold molar excess of DFO-Bz-NCS dissolved in dimethyl sulfoxide in 0.1 M sodium carbonate buffer (pH 9) at 37 °C for 1 h. The resulting DFO-pertuzumab conjugate was purified and buffer exchanged into 1 M HEPES buffer (pH 7.1) using gel filtration spin columns (MWCO 40 kDa, Thermo Fisher Scientific, Rockford, IL). DFO-pertuzumab was radiolabeled with neutralized ^{89}Zr-oxalate using a ratio of 296:1 kBq:μg at 37 °C for 30−60 min for a final pH between 6.8−7.2.[14] ^{89}Zr-pertuzumab with radiochemical yields ≥95% as determined by instant thin-layer chromatography was used for in vitro and in vivo studies without further purification.

ESI-MS Characterization of Chelate Number. DFO-Bz-NCS-pertuzumab conjugate and unmodified pertuzumab were buffer exchanged in 0.25 M NH_4OAc buffer twice using Zeba spin desalting columns (Thermo Scientific, Rockford, IL) following supplier's instructions. The final concentration of protein was quantified using a bicinchoninic acid (BCA) assay (Thermo Scientific, Rockford, IL). A 10 μL aliquot was loaded into an offline electrospray capillary pulled in house using borosilicate tubing on a laser based puller (both B100-58-10 tubing and P-2000 puller were from Sutter Instrument Company, Novato, CA) to perform the native mass spectrometry measurement.[17] The collision energy at the trap and transfer region was adjusted for desolvation of the ions. The pulled capillaries were coated with gold using a sputter coating machine in the Electron Microscopy Core at Washington University in St. Louis. The sample solution was infused to a hybrid ion-mobility quadrupole time-of-flight mass spectrometer (Q-IM-TOF, SYNAPT G2 HDMS, Waters Inc., Milford, MA). The instrument was operated under gentle ESI conditions (capillary voltage 1.5−1.8 kV, sampling cone 20 V, extraction cone 2 V, source temperature 30 °C). The collision energy at the trap and transfer region was adjusted for dissociating the complex. The pressure of the vacuum/backing region was 5.1−5.6 mbar. The instrument was externally calibrated up to 8000 m/z with the clusters produced by ESI of a NaI solution. The peak picking and data processing was performed in Masslynx (v 4.1) and DriftScope software (Water Inc., Milford, MA). The number of DFO per pertuzumab was calculated by (m/z of conjugate − m/z of unconjugated)/(DFO molecular weight) × z, where m/z represents the observed mass to charge ratio and z represents the charge species.

In Vitro Cell Binding Studies. The immunoreactivity of ^{89}Zr-pertuzumab was determined using the Lindmo et al. assay in HER2+ SKBR3 cells.[18] Other cell uptake experiments were performed in HER2+ BT-474 and SKBR3, and HER2− MDA-MB-231 cells, in which 250 μL of 1×10^6 cells/mL were seeded in 24-well plates. Cells were allowed to adhere overnight at 37 °C in a 5% CO_2 atmosphere. The media was removed and replaced with 125 μL of fresh complete media and 125 μL of 50 ng/mL of ^{89}Zr-pertuzumab, saving aliquots in microcentrifuge tubes as a standard. The plates were incubated at 4 °C for 1.5 h, gently rocking. The cells were washed three times with PBS, trypsinized, and transferred to microcentrifuge tubes. Radioactivity associated with cells was counted in a Beckman 8000 gamma counter (Beckman Coulter Inc., Brea, CA). The percentage of bound radioactivity was calculated as the ratio of bound to the total radioactivity added per well multiplied by 100. Equal number of cells per well were confirmed by counting the cells using a Cellometer Auto T-4 Cell Counter (Nexcelom, Lawrence, MA).

Competitive binding assays were performed on SKBR3 cells adhered to 24-well plates as described above. Cells were incubated with 1.7×10^{-10} M ^{89}Zr-pertuzumab in the presence of different concentrations (1.7×10^{-12}−1.7×10^{-6} M) of unlabeled pertuzumab or trastuzumab competitor in triplicate wells at 4 °C for 1.5 h. The cells were washed with PBS and dissociated from the wells as described above and assayed in a gamma counter. The percentage of ^{89}Zr-pertuzumab bound in the presence of competitor/no competitor ($B/B_0 \times 100$) was plotted against the log concentration of added competitor and fitted with a sigmoidal dose−response curve using GraphPad Prism v6 (La Jolla, CA).

Cell internalization assays were modified from previous methods.[19] SKBR3 cells (1×10^6 cells in 400 μL) were seeded into 12-well plates and allowed to adhere overnight in the cell culture incubator. The media was aspirated and replaced with 125 μL of fresh complete media. ^{89}Zr-pertuzumab or ^{89}Zr-trastuzumab positive control antibody[20] was diluted to 50 ng/mL using complete media and 125 μL of each radiolabeled antibody was added to their designated wells. The plates were incubated at 37 °C in a 5% CO_2 atmosphere for 0.5, 1, 3, 17, 24, 28, 42, and 48 h. As a control, some reactions were performed at 4 °C. At each time point, the cells were washed three times with 400 μL of cold PBS and the cells were

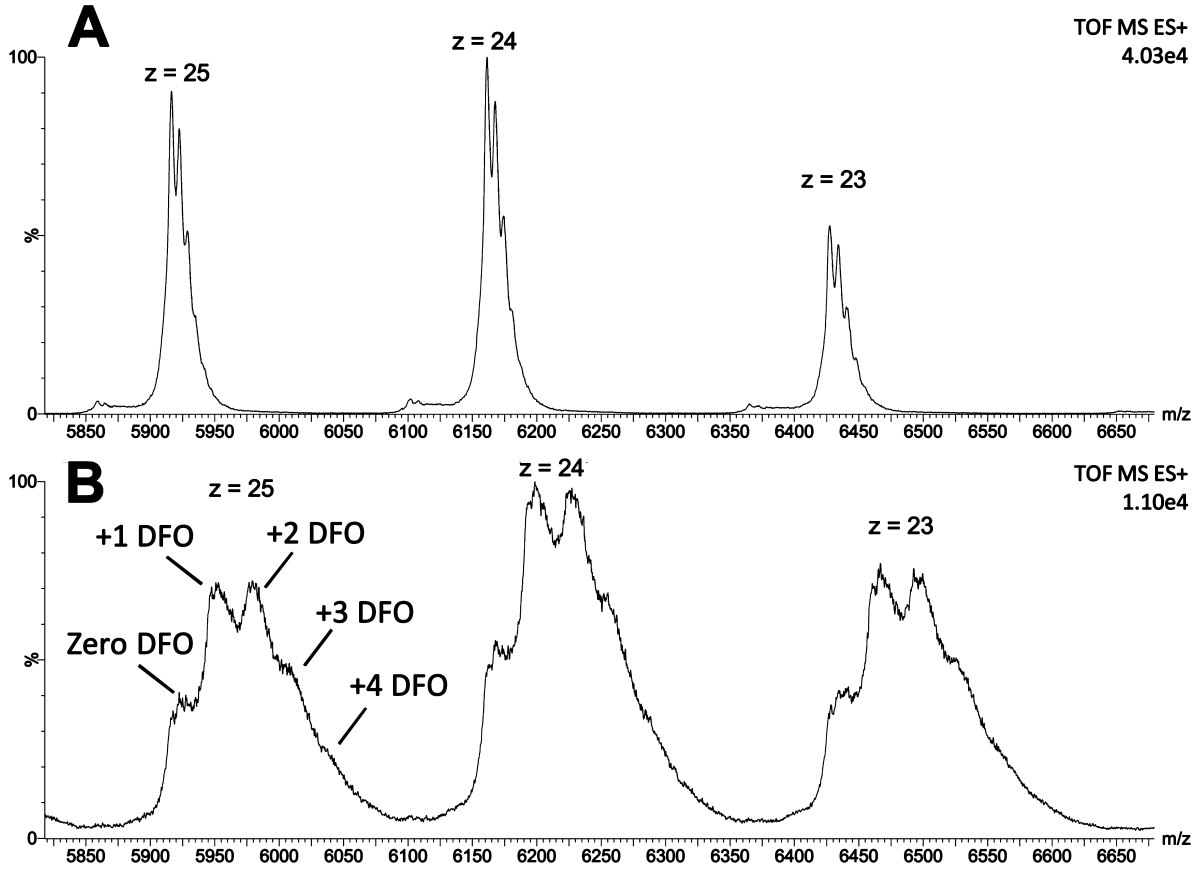

Figure 1. ESI-MS quantified up to four DFO chelates per antibody. (A) Unconjugated pertuzumab depicted in +25, +24, and +23 charge states and (B) DFO-Bz-NCS-pertuzumab conjugate in the same charge states as the unconjugated control.

dissociated from the well via incubation with 400 μL of trypsin for 3 min at 37 °C. The cells were washed again with 200 μL of cold PBS, transferred to a microcentrifuge tube via pipet, and sedimented at 7000*g* using a benchtop centrifuge. The supernatant was collected and the cells were treated with 100 μL of 0.1 M sodium citrate (pH 2) for 5 min to remove any surface bound ^{89}Zr-mAb. The cells were sedimented at 7000*g*, the supernatant was combined with the previously collected supernatant, and assayed in the gamma counter. The amount of ^{89}Zr-mAb bound on the cell surface and internalized was calculated as previously described.[19]

Animal Studies. All animal experiments were conducted according to the guidelines of the Institutional Animal Care and Use Committee (IACUC) and approved by the Washington University Animal Studies Committee. In vivo PET imaging and biodistribution studies were conducted in severely combined immunodeficient female NOG mice (Taconic, Hudson, NY). Mice were inoculated with 150 μL of 1−3 × 10^7 cells/mL (BT-474, SKBR3, and MDA-MB231) suspended in saline with no artificial stimuli.[21] Tumors were allowed to grow for 4−6 weeks until tumors were palpable. Tumor sizes ranged from 4−108 mm^3. Mice were injected via tail-vein with 100 μL of 3.7 MBq of ^{89}Zr-pertuzumab (specific activity 222−296 MBq/mg) in saline. Studies in the presence of unlabeled antibodies were performed with a tail vein injection of 100 μL of 10 mg/mL of either pertuzumab or trastuzumab in saline, between 5−60 min prior to the injection of ^{89}Zr-pertuzumab in the BT-474 xenograft. Static PET images were acquired for 20 min using an Inveon MicroPET/CT scanner (Siemens, Knoxville, TN) at 7 days p.i. The images were reconstructed using maximum a posteriori probability (MAP) algorithm and coregistered with CT images using image display software (Inveon Research Workplace Workstation, Siemens, Schenectady, NY). Regions of interest (ROI) were drawn for tumor uptake and analyzed as standard uptake values (SUV) using the formula SUV = (MBq/mL) × (animal weight (g))/injected dose (MBq). Mice were sacrificed and organs were harvested, weighed, and assayed in the gamma counter for biodistribution studies. Radioactivity associated with each organ was expressed as percentage of injected dose per gram of organ (% ID/g).

Immunohistochemistry. Tumors and spleen were fixed with 4% paraformaldehyde at 4 °C until radioactivity decayed for about 1 week. Tumors were paraffin-embedded, sliced, mounted on slides and stained with hematoxylin and eosin (H&E) by the Washington University Pulmonary Morphology Core facility. HER2 immunohistochemical staining was performed by first blocking the slides with goat serum following instructions from a Vectastain Elite ABC kit (Vector Laboratories, Burlingame, CA) and incubated with 1:200 dilution of a polyclonal goat anti-HER2 antibody (Santa Cruz Biotechnology, Santa Cruz, CA) in PBS for 1 h at room temperature. Secondary antibody incubation was performed following the kit's instructions and colorimetric development was achieved using a 3,3′-diaminobenzidine (DAB) substrate (Vector Laboratories, Burlingame, CA). Tissues were counterstained using tartrazine (yellow) for contrast. Digital images were collected on a Nikon Optiphot-2 microscope equipped with a Zeiss Axiocam digital camera.

Statistical Analysis. Box−Cox analysis indicated that the variances among the test groups were unequal and a logarithm

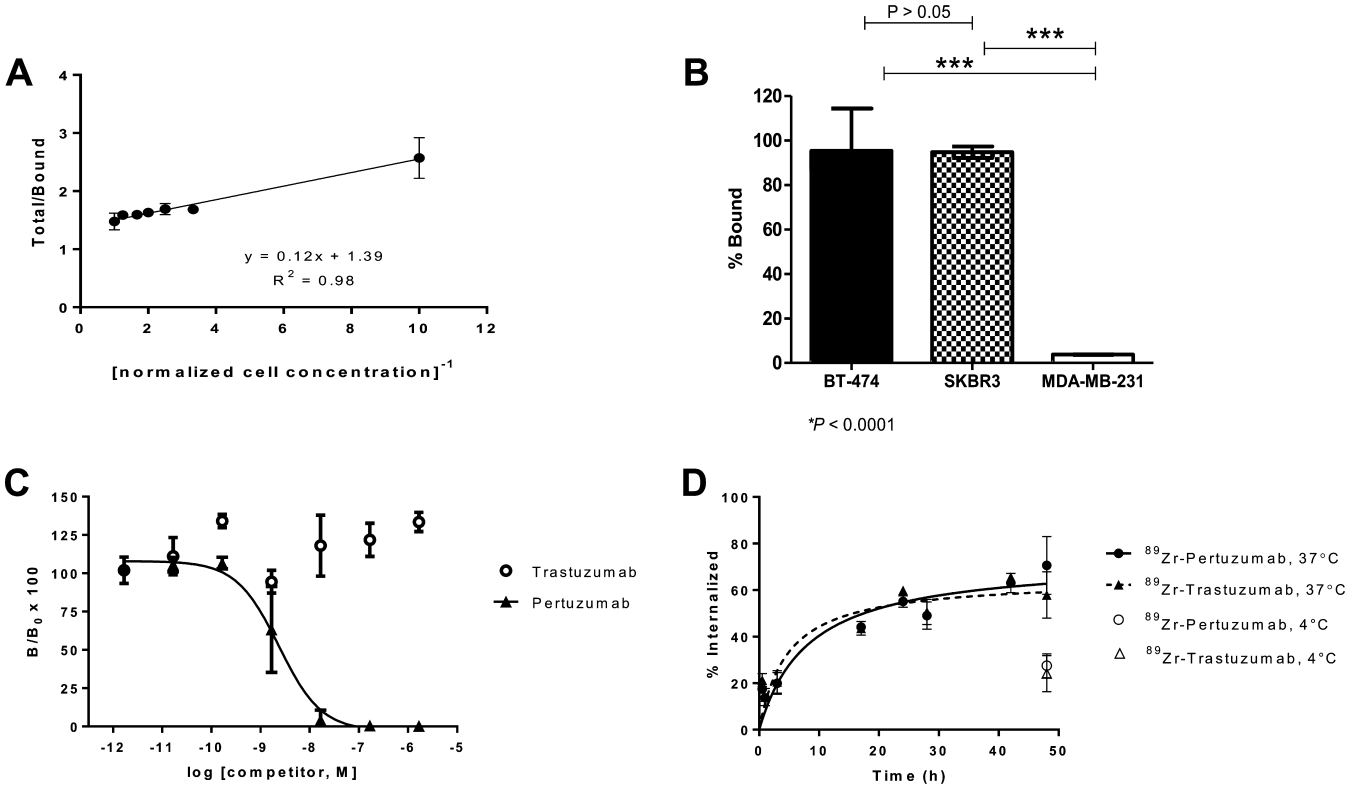

Figure 2. In vitro cell binding studies show ^{89}Zr-pertuzumab retains immunoreactivity and specifically binds to a different HER2 binding site than trastuzumab. Both antibodies internalize at the same rate. (A) Immunoreactivity of ^{89}Zr-pertuzumab in SKBR3 cells was determined with a *y* intercept of 1.39 ± 0.04 and calculated an immunoreactive fraction of 72.2%. (B) Cell uptake studies at 37 °C in BT-474 (HER2+), SKBR3 (HER2+), and MDA-MB-231 (HER2−) demonstrate significantly higher ^{89}Zr-pertuzumab uptake in the HER2+ cell lines compared to the HER2− control ($P < 0.001$). No statistical difference was observed between BT-474 and SKBR3 ($P > 0.05$). (C) Competitive binding studies of ^{89}Zr-pertuzumab with unlabeled pertuzumab in SKBR3 cells at 4 °C yields an EC_{50} of 2.4 ± 0.11 nM, and no competition was observed with unlabeled trastuzumab. (D) Cell internalization studies in SKBR3 cells at 37 °C up to 48 h demonstrate 50% of ^{89}Zr-pertuzumab internalizes at about 20 h, similar to ^{89}Zr-trastuzumab. Control reactions when receptor internalization is reduced at 4 °C show minimal internalization of radiolabeled antibodies at 48 h.

transformation of the SUV and biodistribution data was necessary for variance stabilization.[22] A one-way ANOVA was performed on the log transformation data, followed by group comparisons using the Tukey method to control multiple comparisons. Statistical analysis was performed using GraphPad Prism v6 (GraphPad Software Inc., La Jolla, CA) and SAS v9.3 (SAS Institute, Cary, NC). Although statistical significance was performed on the transformed data, the results are presented in the original metric for ease of discussion.

RESULTS

Chelate Number and Specific Activity of ^{89}Zr-Pertuzumab. The conjugation of DFO-Bz-NCS to pertuzumab was performed by combining 8 mol equiv of chelator at pH 9 for 1 h at 37 °C, followed by immediate purification. ESI-MS determined up to 4 chelates per antibody conjugate, calculated from the mass shift of the unconjugated pertuzumab (Figure 1). Subsequent radiolabeling with ^{89}Zr yielded specific activities of 222−370 MBq/mg with ≥95% radiochemical yield as determined by instant thin layer chromatography.

Cell Binding Studies of ^{89}Zr-Pertuzumab *in Vitro*. The immunoreactivity of ^{89}Zr-pertuzumab was determined using the Lindmo assay in HER2+ SKBR3 cells.[23] The immunoreactive fraction was calculated to be 72.2%, indicating retention of antigen-binding (Figure 2A). The specificity of ^{89}Zr-pertuzumab was investigated in vitro by comparing its binding in HER2+ (SKBR3 and BT-474) and HER2− (MDA-MB-231) cells. Cell binding of ^{89}Zr-pertuzumab to SKBR3, BT-474, and MDA-MB-231 cells was 94.7 ± 2.6, 95.2 ± 19.1, and 3.8 ± 0.1% of total radioactivity added, respectively (Figure 2B). Significantly greater binding was observed in HER2+ compared to HER2− cells ($P < 0.0001$). SKBR3 and BT-474 cells have been reported to have a similar number of HER2 receptors, 6478−11 834 and 10 595−13 917 fmol/mg of protein, respectively.[24] Cell binding studies with ^{89}Zr-pertuzumab in SKBR3 and BT-474 were consistent with Pegram et al. studies,[24] as no statistical difference was observed between SKBR3 and BT-474 cells ($P > 0.05$). SKBR3 cells were thus used for subsequent HER2−binding experiments in vitro. Competitive binding studies showed decreased uptake of the radiolabeled antibody with increasing concentrations of unlabeled pertuzumab, with a half maximal effective concentration (EC_{50}) of 2.4 ± 0.11 nM (Figure 2C). The absence of competitive binding with unlabeled trastuzumab is consistent with an HER2 epitope binding distinction between ^{89}Zr-pertuzumab to domain II and trastuzumab to domain IV of HER2.[4,10] Furthermore, the binding of ^{89}Zr-pertuzumab is increased by 30% in the presence of high concentrations (0.02−2 μM) of unlabeled trastuzumab. This observation is also in agreement with the in silico studies by Fuentes et al. in which HER2 conformational changes occur upon trastuzumab binding resulting in the increased affinity of pertuzumab for its

dx.doi.org/10.1021/mp500323d | *Mol. Pharmaceutics* 2014, 11, 3988−3995

HER2 binding epitope.[10] Lastly, a comparative rate of cellular internalization study was conducted at 37 °C with ^{89}Zr-pertuzumab and ^{89}Zr-trastuzumab. The internalization of both antibodies was similar; with 50% of ^{89}Zr-pertuzumab internalizing at 23 h and ^{89}Zr-trastuzumab at 21 h (Figure 2D). The control reactions at 4 °C when receptor internalization is reduced showed minimal internalization of both radiolabeled antibodies at 48 h and demonstrated the efficiency of the acid wash treatment to separate surface-bound from internalized antibody. These studies showed ^{89}Zr-pertuzumab was as effective as ^{89}Zr-trastuzumab in binding HER2 in vitro, despite different binding sites.

PET Imaging and Biodistribution of ^{89}Zr-Pertuzumab in Breast Cancer Xenografts. Subcutaneous tumor xenografts in severely combined immunodeficient mice have been reported to have excellent tumor take rates without the need for exogenous stimuli such as matrigel or estrogen pellets.[21] We observed slow tumor growth for BT-474 and MDA-MB-231, which was achieved in 4−6 weeks with tumor take rates of 93% (13/14) and 100% (7/7), respectively. The SKBR3 tumor take rate, even at high cell concentration (1×10^8 cells/mL) was 22% (3/14) and this low sampling hampered our investigation of ^{89}Zr-pertuzumab in this model.

Quantitative PET imaging was performed at 7 days p.i., in BT-474 xenografts and ^{89}Zr-pertuzumab accumulation in the BT-474 tumor was higher than in MDA-MB-231 with max SUV of 10.5 ± 6.1, and 2.2 ± 0.8, respectively (P = 0.0006, Figure 3A, B). These data were analyzed as the logarithmic transformation to more precisely represent the means due to the high variances observed. Max SUV analysis showed increased tumor uptake of ^{89}Zr-pertuzumab in BT-474 in the presence of unlabeled trastuzumab (19.0 ± 5.4) although not statistically significant (P > 0.05) and may be attributed to the high variance in each test group. The accumulation of ^{89}Zr-pertuzumab was reduced in the presence of unlabeled pertuzumab with SUV of 2.2 ± 2.5 (P = 0.0004), a value equivalent to the tumor uptake in the MDA-MB-231 model (P > 0.05). Post-PET biodistribution studies significantly correlate with PET imaging quantification yielding Pearson's coefficient of r = 0.98, with a linear fit of R^2 = 0.98 (P = 0.01, Supporting Information Figure S1). The tumor uptake was higher for BT-474 with 47.5 ± 32.9% ID/g (n = 7) compared to the MDA-MB-231 xenograft with 9.5 ± 1.7% ID/g (n = 7, P = 0.0009). Blocking with unlabeled pertuzumab had a significant reduction in tumor uptake, 8.5 ± 6.6% ID/g (n = 4, P = 0.0006). The tumor accumulation of ^{89}Zr-pertuzumab showed a significant increase of 173 ± 74.5% ID/g in the presence of unlabeled trastuzumab (n = 3, P = 0.01). The variance instability for the biodistribution studies is shown in Supporting Information Figure S2, showing the need to perform statistical analyses on the logarithmic transformations of the data.[22] Figure 4 shows the biodistribution of ^{89}Zr-pertuzumab at 7 days p.i. Low accumulation was observed in most normal organs particularly the blood, muscle, and heart with 0.05 ± 0.02, 0.7 ± 0.2, and 1.0 ± 0.1% ID/g, respectively, for the BT-474 xenografts.

Interestingly, the spleen showed a relatively high tracer accumulation, greater than 100% ID/g, in these severely combined immunodeficient mice. This unexpected outcome led us to investigate whether this phenomenon was a consequence of these tumors; thus, we performed biodistribution studies of ^{89}Zr-pertuzumab in nontumor bearing NOGs and in the conventional athymic *Nu/Nu* mice as a control. Similar spleen uptake of 119.7 ± 17.9% ID/g (n = 2) was observed in

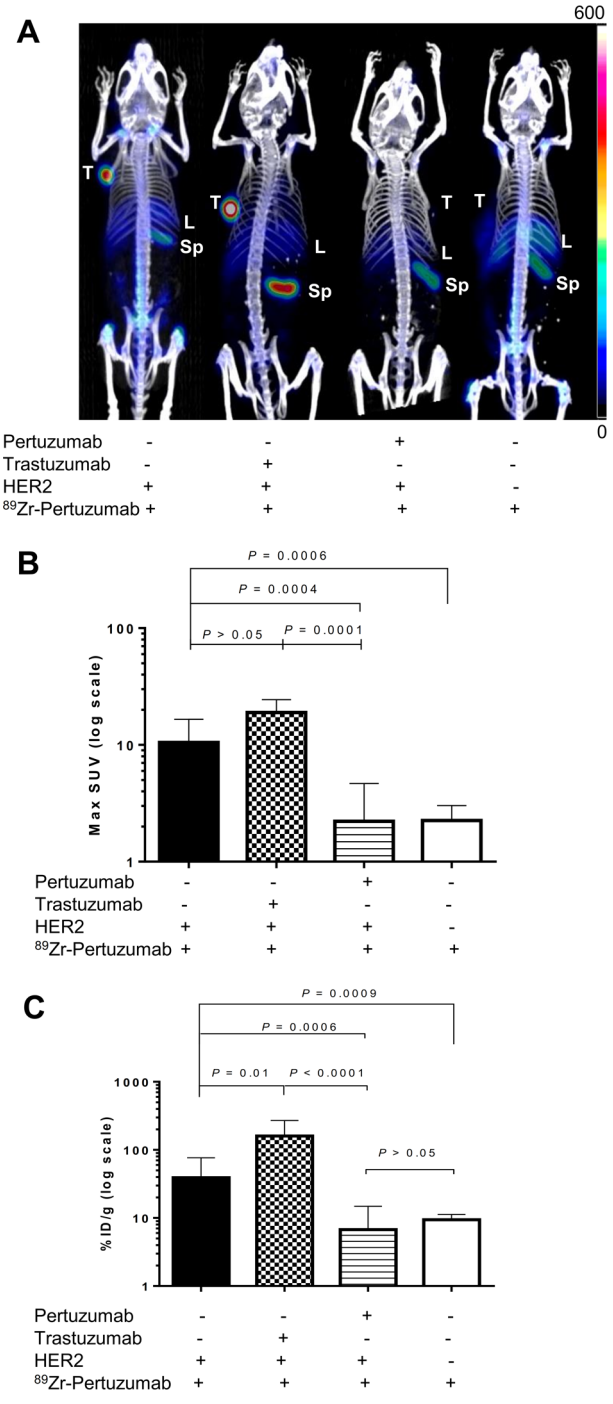

Figure 3. In vivo studies show high and specific tumor uptake of ^{89}Zr-pertuzumab in HER2+ tumors, enhanced in the presence of trastuzumab. (A) Maximum intensity projection of PET/CT images of ^{89}Zr-pertuzumab in BT-474 (HER2+) and MDA-MB-231 (HER2−) breast cancer xenografts at 7 days p.i. The scale bar is from 0−600 kBq/mL. (B) Max SUV quantification of ^{89}Zr-pertuzumab tumor uptake in BT-474 was 10.5 ± 6.1, increased in the presence of unlabeled trastuzumab (19.0 ± 5.4), decreased in the presence of a blocking concentration of unlabeled pertuzumab (2.2 ± 2.5), and decreased in MDA-MB-231 xenografts (2.2 ± 0.8). (C) Biodistribution studies correlate with PET imaging quantification with 47.5 ± 32.9% ID/g for ^{89}Zr-pertuzumab in BT-474, 173 ± 74.5% ID/g in the presence of unlabeled trastuzumab (P = 0.01), 8.5 ± 6.6% ID/g in the presence of unlabeled pertuzumab (P = 0.0006), and 9.5 ± 1.7% ID/g in the HER2− MDA-MB-231.

dx.doi.org/10.1021/mp500323d | *Mol. Pharmaceutics* 2014, 11, 3988−3995

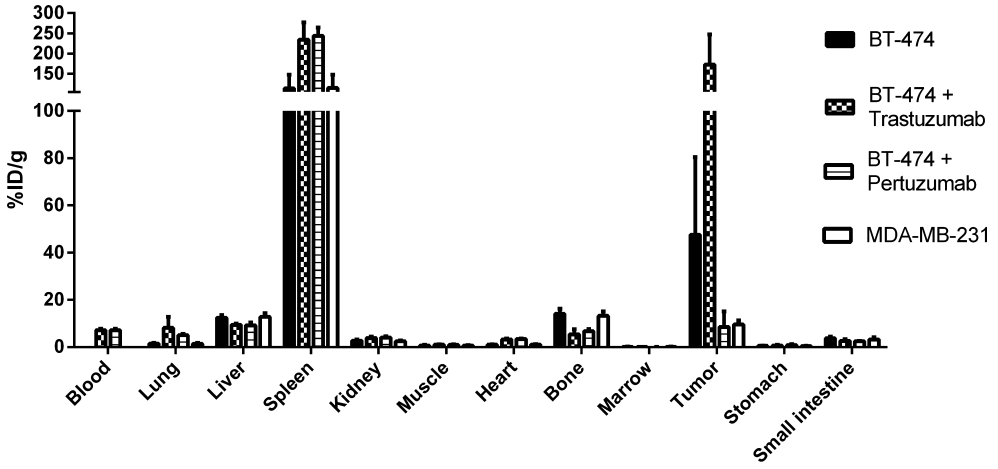

Figure 4. Biodistribution of ^{89}Zr-pertuzumab in HER2+ BT-474 and HER2− MDA-MB-231 xenografts. All mice were injected with ^{89}Zr-pertuzumab. A cohort of BT-474 xenografts were coinjected with either unlabeled trastuzumab (checkered bars) or unlabeled pertuzumab (horizontal line bars). ^{89}Zr-pertuzumab alone with no other cotreatments added were studied in BT-474 (black bars) or MDA-MB-231 (unfilled bars).

nontumor bearing NOG mice at 7 days p.i. However, only 2.7 ± 1.7% ID/g (n = 2) was observed in nontumor bearing athymic *Nu/Nu* mice (Supporting Information Figure S3). Thus, the high spleen uptake is unique to the severely combined immunodeficient mice. We hypothesize that the absence of immunogenic response (e.g., the lack of T, B, and natural killer cell functions) as well as the abnormal macrophage activity in the NOG strain are involved in the catabolism of ^{89}Zr-pertuzumab to the spleen. In contrast, conventional strains of mice that still have some intact immunogenic response (e.g., with functional natural killer cells), catabolize antibodies primarily in the liver.[25−27] Further investigations are needed to determine the pharmacokinetic properties of humanized antibodies in different types of preclinical models.

Histology and Immunohistochemistry. Following biodistribution studies, tumor slices from the BT-474 and MDA-MB-231 groups were stained for HER2 expression (brown) using a commercially available anti-HER2 antibody and counterstained with tartrazine (yellow) (Supporting Information Figure S4). HER2 expression in BT-474 tumors was pronounced, visibly outlining the HER2 extracellular membrane, whereas the MDA-MB-231 tissue stained negative for HER2 expression. Furthermore, we observed negative HER2 staining in the spleen, confirming the absence of human HER2 in this organ (data not shown). H&E stains confirmed tumor viability. These results showed that the specific targeting of ^{89}Zr-pertuzumab to HER2 in vivo were in agreement with the HER2 expression levels ex vivo.

DISCUSSION

Our findings illustrate ^{89}Zr-pertuzumab specifically accumulates in HER2+ tumors, enhanced by the presence of trastuzumab. This study is consistent with in silico studies conducted by Fuentes et al., where a conformational change in HER2 occurs upon trastuzumab binding, likely inducing greater exposure of this binding site leading to the enhanced affinity of pertuzumab.[10] Our in vitro and in vivo studies show increased cellular and tumor uptake of ^{89}Zr-pertuzumab in the presence of excess unlabeled trastuzumab, respectively (Figure 2C, Figure 3). These different studies did not show a comparable degree of enhanced uptake of ^{89}Zr-pertuzumab, with only 30% increased cellular uptake in vitro at 4 °C within 1.5 h of incubation and almost 400% increased tumor uptake in vivo within 7 days of bloodstream circulation. This apparent discrepancy may be due to differences in the kinetic properties of ^{89}Zr-pertuzumab in the more artificial environment in vitro compared to the complex environment in vivo over several days. The 7 day PET imaging after administration of ^{89}Zr-pertuzumab was performed to allow clearance of the radiolabeled antibody as exemplified by previously studied ^{89}Zr-labeled monoclonal antibodies, one of the advantages of imaging with ^{89}Zr over shorter-lived radioisotopes.[5,16,28,29] An earlier imaging time point at 5 days p.i. was performed in a small cohort of mice, and no differences in tumor uptake were observed between 5 and 7 days p.i. (data not shown), which confirms the in vivo stability of this radiopharmaceutical.

Additionally, the increased bloodstream residence of ^{89}Zr-pertuzumab may also contribute to its increased tumor uptake in the presence of trastuzumab. The absence of T, B, and NK cells part of the immune response and the abnormal macrophage activity in this NOG host may contribute to the inefficiency of the clearance mechanism for antibodies,[21,28] as evidenced by the high spleen uptake of ^{89}Zr-pertuzumab. In contrast, the less immunocompromised strains such as athymic mice which require estrogen pellet implantation for BT-474 tumor engraftment have some functional immunogenic response to mediate the hepatobiliary clearance of antibodies more efficiently.[25−27] As such, higher liver and lower spleen uptake were observed for nontumor bearing athymic mice compared to the NOG strain (Supporting Information Figure S3). Differences in clearance mechanisms for antibodies in different preclinical models may be an interesting future study; however, this should not impede the translation of ^{89}Zr-pertuzumab to clinical trials.

In a previous study, Scheuer et al. investigated pertuzumab as an optical imaging agent labeled with a Cy5 fluorescent dye, to assess the synergistic therapeutic effect of the combination of pertuzumab and trastuzumab in KPL-4 human breast cancer xenografts.[9] This study found similar tumor uptake between Cy5-pertuzumab alone and Cy5-pertuzumab in combination with unlabeled trastuzumab. No enhancement of Cy5-pertuzumab tumor uptake in the presence of trastuzumab was

reported, possibly due to differences in experimental conditions such as the increased injected mass of the Cy5-pertuzumab, in which its unlabeled fraction may block some HER2 binding sites or the reduced sensitivity of optical imaging compared to PET.

A limitation of our study is the high variance in ^{89}Zr-pertuzumab tumor uptake in the BT-474 xenografts. This observation may be a consequence of tumor growth variability among the NOGs. Despite the high variance in the means, ^{89}Zr-pertuzumab demonstrates high affinity and selectivity for HER2+ tumors in vivo. Although radiolabeled trastuzumab has had much success in imaging HER2 expression in breast cancer patients who were trastuzumab naïve or were undergoing trastuzumab therapy,[3,5] radiolabeled pertuzumab may be a more favorable alternative as it binds to a distinct HER2 epitope. Imaging with pertuzumab while treating with trastuzumab or the trastuzumab antibody drug conjugate, T-DM1, would allow a noncompetitive and cooperative binding interaction with HER2. Currently, ^{111}In-labeled pertuzumab is being investigated in breast cancer patients using single-photon emission computed tomography;[6] however, the sensitivity of PET and the resolution of ^{89}Zr will provide excellent images with reduced radioactivity exposure to the patient. Thus, PET imaging using ^{89}Zr-pertuzumab may be advantageous to monitor patient response to HER2-targeted therapy involving trastuzumab to more sensitively detect HER2 expression.

CONCLUSIONS

^{89}Zr-pertuzumab as a PET imaging agent detects HER2 expression selectively in breast cancer xenograft models with increased tumor uptake in the presence of trastuzumab. ^{89}Zr-pertuzumab is a promising radiopharmaceutical for noninvasive imaging of HER2+ breast cancer undergoing trastuzumab therapy to enhance the sensitivity of HER2 detection in vivo.

ASSOCIATED CONTENT

Supporting Information

Supplemental Figure 1 depicts the correlation between biodistribution and max SUV data. Supplemental Figure 2 depicts a sample variance analysis of the biodistribution data. Supplemental Figure 3 depicts the biodistribution of ^{89}Zr-pertuzumab in nontumor-bearing NOG and athymic *Nu/Nu* mice. Supplemental Figure 4 depicts the immunohistochemical analysis of BT-474 and MDA-MB-231 tumors for HER2 expression. This material is available free of charge via the Internet at http://pubs.acs.org.

AUTHOR INFORMATION

Corresponding Author

*E-mail: lapis@mir.wustl.edu. Phone: (314) 362-4696. Fax: (314) 362-9940. Address: Mallinckrodt Institute of Radiology, Washington University School of Medicine, Campus Box 8225, 510 South Kingshighway Boulevard, St. Louis, MO 63110, United States.

Notes

The authors declare no competing financial interest.

ACKNOWLEDGMENTS

This work was supported in part by the DOE BER Integrated Research Training Program of Excellence in Radiochemistry under grants DESC0002032 and DESC0008432. We thank Drs. Weidong Cui and Hao Zhang from the NIH/NIGMS Mass Spectrometry Resource (P41GM103422) at Washington University in St. Louis (WUSTL) for acquiring the mass spectra and helpful discussions, the WUSTL Isotope Production Team for producing ^{89}Zr, the WUSTL Small Animal Imaging Facility for PET imaging and biodistribution studies, Tim Whitehead and Kathryn Trinkaus for statistical analysis, the WUSTL Pulmonary Morphology Core Facility for embedding and H&E staining of tissues, and Dr. Ron Bose for helpful discussions. The authors wish to acknowledge the support of Kathryn Trinkaus of the Biostatistics Core, Siteman Comprehensive Cancer Center, and NCI Cancer Center Support Grant P30 CA091842.

ABBREVIATIONS

HER2, human epidermal growth factor receptor-2; PET, positron emission tomography; ^{89}Zr, zirconium-89; DFO-Bz-NCS, desferrioxamine-*p*-benzyl-isothiocyanate; DFO-Bz-NCS-pertuzumab, desferrioxamine conjugated to pertuzumab; ^{89}Zr-pertuzumab, ^{89}Zr-labeled DFO-Bz-NCS-pertuzumab conjugate; NOG, severely combined immunodeficient mice with Rag2$^{-/-}$ and Il2rg$^{-/-}$ knockout genes

REFERENCES

(1) Gaykema, S. B.; Brouwers, A. H.; Lub-de Hooge, M. N. ^{89}Zr-bevacizumab PET imaging in primary breast cancer. *J. Nucl. Med.* **2013**, *54*, 1014−1018.

(2) Osborne, J. R.; Green, D. A.; Spratt, D. E. A Prospective Pilot Study of ^{89}Zr-J591/PSMA Positron Emission Tomography (PET) in Men with Localized Prostate Cancer Undergoing Radical Prostatectomy. *J. Urol.* **2013**, 1439−1445.

(3) Dijkers, E. C.; Oude Munnink, T. H.; Kosterink, J. G.; et al. Biodistribution of ^{89}Zr-trastuzumab and PET imaging of HER2−positive lesions in patients with metastatic breast cancer. *Clin. Pharmacol. Ther.* **2010**, *87*, 586−592.

(4) Capelan, M.; Pugliano, L.; De Azambuja, E. Pertuzumab: new hope for patients with HER2−positive breast cancer. *Annals Oncol.* **2013**, 273−282.

(5) Tamura, K.; Kurihara, H.; Yonemori, K.; et al. 64Cu-DOTA-trastuzumab PET imaging in patients with HER2−positive breast cancer. *J. Nucl. Med.* **2013**, *54*, 1869−1875.

(6) Imaging With 111 Indium (111In)-pertuzumab (PmAb) to Predict Response to trastuzumab (TmAb) in Human Epidermal Growth Factor-2 (HER2) Positive Metastatic Breast Cancer (MBC) (PETRA): Ontario Clinical Oncology Group, 2013. ClinicalTrials.gov (accessed June 2014).

(7) McLarty, K.; Cornelissen, B.; Cai, Z.; et al. Micro-SPECT/CT with 111In-DTPA-pertuzumab sensitively detects trastuzumab-mediated HER2 downregulation and tumor response in athymic mice bearing MDA-MB-361 human breast cancer xenografts. *J. Nucl. Med.* **2009**, *50*, 1340−1348.

(8) Persson, M.; Gedda, L.; Lundqvist, H.; et al. [177Lu]pertuzumab: Experimental Therapy of HER-2−Expressing Xenografts. *Cancer Res.* **2007**, *67*, 326−331.

(9) Scheuer, W.; Friess, T.; Burtscher, H.; Bossenmaier, B.; Endl, J.; Hasmann, M. Strongly enhanced antitumor activity of trastuzumab and pertuzumab combination treatment on HER2−positive human xenograft tumor models. *Cancer Res.* **2009**, *69*, 9330−9336.

(10) Fuentes, G.; Scaltriti, M.; Baselga, J.; Verma, C. Synergy between trastuzumab and pertuzumab for human epidermal growth factor 2 (Her2) from colocalization: an in silico based mechanism. *Breast Cancer Res.* **2011**, *13*, R54.

(11) Wooten, A.; Madrid, E.; Schweitzer, G.; et al. Routine Production of ^{89}Zr Using an Automated Module. *Appl. Sci.* **2013**, *3*, 593−613.

(12) Verel, I.; Visser, G. W.; Boellaard, R.; Stigter-van Walsum, M.; Snow, G. B.; van Dongen, G. A. ^{89}Zr immuno-PET: comprehensive

procedures for the production of ^{89}Zr-labeled monoclonal antibodies. *J. Nucl. Med.* **2003**, *44*, 1271−1281.
(13) Holland, J. P.; Sheh, Y.; Lewis, J. S. Standardized methods for the production of high specific-activity zirconium-89. *Nucl. Med. Biol.* **2009**, *36*, 729−739.
(14) Perk, L. R.; Vosjan, M. J.; Visser, G. W.; et al. p-Isothiocyanatobenzyl-desferrioxamine: a new bifunctional chelate for facile radiolabeling of monoclonal antibodies with zirconium-89 for immuno-PET imaging. *Eur. J. Nucl. Med. Mol. Imaging* **2010**, *37*, 250−259.
(15) Vosjan, M. J.; Perk, L. R.; Visser, G. W.; et al. Conjugation and radiolabeling of monoclonal antibodies with zirconium-89 for PET imaging using the bifunctional chelate p-isothiocyanatobenzyl-desferrioxamine. *Nat. Protoc.* **2010**, *5*, 739−743.
(16) Ikotun, O. F.; Marquez, B. V.; Huang, C.; et al. Imaging the L-type amino acid transporter-1 (LAT1) with Zr-89 immunoPET. *PLoS One* **2013**, *8*, e77476.
(17) Zhang, H.; Cui, W.; Gross, M. L. Mass spectrometry for the biophysical characterization of therapeutic monoclonal antibodies. *FEBS Lett.* **2014**, *588*, 308−317.
(18) Lindmo, T.; Boven, E.; Cuttitta, F.; Fedorko, J.; Bunn, P. A., Jr. Determination of the immunoreactive fraction of radiolabeled monoclonal antibodies by linear extrapolation to binding at infinite antigen excess. *J. Immunol. Methods* **1984**, *72*, 77−89.
(19) Lub-de Hooge, M. N.; Kosterink, J. G. W.; Perik, P. J.; et al. Preclinical characterisation of In-111-DTPA-trastuzumab. *Br. J. Pharmacol.* **2004**, *143*, 99−106.
(20) Chang, A. J.; Desilva, R.; Jain, S.; Lears, K.; Rogers, B.; Lapi, S. ^{89}Zr-Radiolabeled trastuzumab Imaging in Orthotopic and Metastatic Breast Tumors. *Pharmaceuticals (Basel)* **2012**, *5*, 79−93.
(21) Nanni, P.; Nicoletti, G.; Palladini, A.; et al. Multiorgan Metastasis of Human HER-2+ Breast Cancer in Rag2−/−;Il2rg−/− Mice and Treatment with PI3K Inhibitor. *PLoS One* **2012**, *7*, e39626.
(22) Box, G. E. P.; Hunter, W. G.; Hunter, J. S. 7.8 Simplification and Increased Sensitivity from Transformation. *Statistics for Experimenters: An Introduction to Design, Data Analysis, and Model Building*; John Wiley and Sons, Inc: Canada, 1978; pp 231−238.
(23) Lindmo, T.; Boven, E.; Cuttitta, F.; Fedorko, J.; Bunn, P. A., Jr Determination of the immunoreactive function of radiolabeled monoclonal antibodies by linear extrapolation to binding at infinite antigen excess. *J. Immunol. Methods* **1984**, *72*, 77−89.
(24) Pegram, M. D.; Konecny, G. E.; O'Callaghan, C.; Beryt, M.; Pietras, R.; Slamon, D. J. Rational Combinations of trastuzumab With Chemotherapeutic Drugs Used in the Treatment of Breast Cancer. *J. Natl. Cancer Inst.* **2004**, *96*, 739−749.
(25) Moldoveanu, Z.; Epps, J. M.; Thorpe, S. R.; Mestecky, J. The sites of catabolism of murine monomeric IgA. *J. Immunol.* **1988**, *141*, 208−213.
(26) Henderson, L. A.; Baynes, J. W.; Thorpe, S. R. Identification of the sites of IgG catabolism in the rat. *Arch. Biochem. Biophys.* **1982**, *215*, 1−11.
(27) Ferl, G. Z.; Kenanova, V.; Wu, A. M.; DiStefano, J. J., 3rd A two-tiered physiologically based model for dually labeled single-chain Fv-Fc antibody fragments. *Mol. Cancer Ther.* **2006**, *5*, 1550−1558.
(28) Sham, J. G.; Kievit, F. M.; Grierson, J. R.; et al. Glypican-3-Targeted ^{89}Zr PET Imaging of Hepatocellular Carcinoma. *J. Nucl. Med.* **2014**, *13*, 13.
(29) Sugyo, A.; Tsuji, A. B.; Sudo, H.; et al. Evaluation of ^{89}Zr-Labeled Human Anti-CD147 Monoclonal Antibody as a Positron Emission Tomography Probe in a Mouse Model of Pancreatic Cancer. *PLoS One* **2013**, *8*, e61230.